



Investigation of an adsorbent based on novel starch/chitosan nanocomposite in extraction of indigo carmine dye from aqueous solutions

Salah Fawzi Abdellah Ali ^{1,2} , Ehab Said Gad ^{1,3} 

¹Chemistry Department, College of Science and Arts, Jouf University, Saudi Arabia

²Materials Science Department, Institute of Graduate Studies & Research, Alexandria University, Egypt

³Department of Chemistry, Faculty of Science, Al-Azhar University, Nasr City

*corresponding author e-mail address: salah15eg@yahoo.com | Scopus ID [57191369963](https://orcid.org/0000-0001-9141-1111)

ABSTRACT

Treatment of corn starch using pullulanase to prepare high yield of starch nanoparticles (StNPs) in a short time is one of the best ways of green industry of StNPs in comparison with other preparation procedures. Morphology of surface, particle size, function groups behavior and crystalline structure were investigated by using Scanning electron microscope (SEM), Dynamic light scattering (DLS), Transmission electron microscope (TEM), Fourier transforms infrared spectroscopy and X-ray diffraction. Starch nanoparticles can be used with chitosan to generate a novel composite to remove dyes from aqueous solutions. Indigo carmine dye was remediated with chitosan starch nanoparticle composite to evaluate the adsorption efficiency of such composite. Batch experiments were done to check the optimum pH, contact time, adsorbent dose, initial dye concentration and temperature to assess the kinetic data from isotherm of adsorption. The obtained results are fitted with pseudo second order and Langmuir isotherms. Free Gibbs energy (ΔG°), enthalpy (ΔH°) and entropy (ΔS°) of the sorption parameters indicated spontaneous and endothermic adsorption process.

Keywords: Starch nanoparticles StNPs; Indigo carmine; Chitosan-StNPs composite; Thermodynamics; adsorption process.

1. INTRODUCTION

Natural polymers are considered to be the most favorite class of polymers in the preparation of biodegradable nanoparticles that have attracted researchers in recent years. Starch is a natural polymer which nominee for making nanocrystals and nanoparticles [1,2]. Starch has many features among other natural polymers (abundant, inexpensive, renewable, nontoxic and environment friendly). A large amount of starch is produced in stabilized crops like (potato, wheat, maize, rice and cassava). A starch molecule is composed of anhydrous glucose units that are typically forming the distinctive granules. Starch granules are made up of plentiful nano-sized semi-crystalline blockets. Nano-blockets could be secluded from starch via moderate hydrolysis using acids and/or enzymes. Starch is composed of amylose and amylopectin that are different in the structure chain. Amylose consists of glucose units linked together by α -(1-4) glucosidic bond and molecular weight nearly a million. Amylopectin is linear chain of glucose units linked together by α -(1-4) glucosidic bond and branches linked by α -(1-6) glucosidic bond and molecular weight up to hundred millions. A universal review on starch nanoparticle preparation, characterization and applications was published recently [3].

Starch nanoparticles have attracted researchers in the last decades because of lone physicochemical properties as compared with native starch [4]. Starch nanoparticles have promising future in many industrial applications as antioxidant [5], packaging and papermaking industry [1,6], carrier in drugs [7,8], adsorbent in waste water treatment [9,10] and slow release fertilizer [11]. The enzymolysis procedure is one of the best ways of starch nanoparticles preparation and producing large yield in short duration in green chemistry when compared with acid hydrolysis. Chitosan is another promising biodegradable, biocompatible polymer and has been investigated by several researchers for different applications [12]. Chitosan has been used as an efficient adsorbent of heavy metal ions and dyes because of its high chelating ability and low cost [13]. Composites of starch and chitosan were prepared and found to have unique physio-chemical properties in various applications [14-16]. In this work, starch nanoparticles from corn starch using pullulanase as isoamylase by self-assembly at 4 °C mechanism was prepared [4]. A novel good adsorbent of starch nanoparticles with chitosan can be used to remove indigo carmine dye in aqueous solutions.

2. MATERIALS AND METHODS

2.1. Materials.

Corn starch was obtained from Egyptian starch and glucose Company ESGC, Pullulanase (E.C.3.2.1.41, 1000 ASPU/g, and 1.15 g/mL) was supplied by GENENCORE, Chitosan of molecular weight $1-3 \times 10^5$ g / mol with deacetylation degree between 75-85% and 200-800 cPs, hydrochloric acid, caustic soda and disodium hydrogen phosphate were obtained from Sigma Aldrich. All supplied chemicals are analytical grade.

2.2. Preparation of starch nanoparticles.

Starch slurry 5 % was prepared in buffer solution (pH = 5.0) and stirred for 30 min. in boiling water bath till gelatinized starch obtained. The temperature was adjusted at 58 °C to add the enzyme 30 ASPU/ g starch to start reaction of de-branching for 8 hrs. The reaction was stopped by heating at 100 °C for 30 min to inactivate the pullulanase. The slurry was cooled to room temp

then stored at 4 °C for 8 hrs then washed by distilled water and centrifuged 4 times till neutrality then freeze drying was used [4].

2.3. Chitosan/StNPs composite preparation.

2 gm of chitosan in 100 ml 2 % acetic acid was prepared and stirred till homogeneity. 2 gm of starch nanoparticles in 100 ml distilled water was heated till gelatinized in boiling water bath for 30 min. then cool for 5 min. The two solutions were mixed in 250 ml beaker and stirred for 30 min. at room temperature then dried at 70 °C for 12 hrs in a Petri dish [13].

2.4. Characterization.

2.4.1. Scanning electron microscopy (SEM).

Samples of native starch and StNPs were observed using Quanta 250 FEG(Field Emission Gun) scanning electron microscope at 30 kV accelerating voltage. Micrographs of native starch and StNPs were presented at 3000 and 30000 magnification respectively.

2.4.2. Transmission electron microscopy (TEM).

Transmission electron micrographs of StNPs were taken with a JOEL-JEM 1010 transmission electron microscope (Made in Japan) with an acceleration voltage of 80 kV. StNPs were deposited on a carbon-coated grid without any treatments.

2.4.3. X-ray diffraction (XRD).

Native corn starch and StNPs samples were stored for 24 hrs. in a sealed container at a relative humidity of 85 % to achieve constant moisture content. XRD patterns were measured at room temperature. A Siemens D-5000 diffractometer (BRUKER, D8, Germany) using Cu Ka radiation ($k = 1.543$) and a secondary beam graphite monochromator was operated at 40 kV and 30 mA. Intensities were measured in the 4–45 2θ range with a 0.03 step size and measuring time of 2.0 s per point.

2.4.4. Dynamic light scattering (DLS).

The size of StNPs was determined using DLS at room temperature on a Plus particle size analyzer (Nicomb Instruments Corporation) at the 90 scattering angle (Calif., USA). All solutions were filtered using disposable 0.45 μm pore filters before analysis at 1.0 mg/ml concentration.

2.4.5. Fourier transforms infrared spectroscopy (FTIR).

Fourier transform infrared spectra of corn starch and StNPs were acquired on an FTIR spectra (Japan-JASCO 4600) using KBr disk technique. For FTIR measurement, the samples were mixed with anhydrous KBr and then compressed into thin disk-shaped

pellets. The spectra were obtained with a resolution of 2 cm⁻¹ between wave number ranges of 4000–400 cm⁻¹. The assumed line shape was Lorentzian with a half-width of 19 cm⁻¹ and a resolution enhancement factor of 1.9.

2.5. Adsorbate preparation and calibration.

Stock solution of Indigo carmine IC was prepared by dissolving 0.125 g in 500 mL of distilled water to obtain 250 mg/L dye concentration solution. The working concentrations were prepared by diluting 250 mg/L predetermined volumes of the stock solution accurately to known initial concentrations of 20, 40, 60, 80, 100, 125, 175 and 225 mg/L. A calibration curve of the IC dye was first prepared via serial dilution and absorbance determined using a UV-spectrophotometer (T80+ UV/Vis spectrometer) at λ_{max}=612 nm. All absorbance readings are measured in duplicate and the average absorbance values of IC dye calculated.

2.6. Batch sorption examination.

Examination of Sorption through single batch reactor systems were carried out and the effects of different parameters such as; Ch-StNPs composite dosage (10-50 mg), pH (2.5-8.5), initial dye concentration (20-225 mg/L), temperature (25-55 °C) and effect of contact time (10-300 min.) were studied. The sorption experiments were performed at a constant agitation speed of 300 rpm using 50 mL beaker containing 20ml of IC dye solution of known concentrations. Solutions pH was adjusted with either 0.1M HCl or NaOH. Determination of equilibrium between Ch-StNPs composite and IC dye by shaken the beaker for different time intervals till reach an adequate time. Ch-StNPs composite Sorption capacity screened at known time intervals to measure the residual IC dye concentration using UV-Vis spectrophotometer at λ_{max} of 612 nm. The quantity of IC dye absorbed at equilibrium was then determined using Eq. (1)

$$q_e = (C_0 - C_e) \times V / M \quad (1)$$

where, q_e (mg/g) is the equilibrium adsorption capacity of adsorbed IC dye onto Ch-StNPs composite, C_0 (mg/L) the initial concentration of IC dye, C_e (mg/L) the equilibrium concentrations of IC dye at time (t) in liquid phase, V (L) the volume of IC dye solution and M (g) the mass of Ch-StNPs composite used. The percentage of IC dye removal was also calculated using Eq. (2)

$$\text{Removal \%} = (C_0 - C_e) / C_0 \times 100 \quad (2)$$

3. RESULTS

3.1. Characterization of StNPs and Chitosan/StNPs composite.

3.1.1. Native starch and StNPs morphology.

The SEM & TEM images showed the round and polyhedral shape of the native starch and StNPs as obtained from several other studies [1]. The SEM images found in Figure 1 (a, b) indicate that the native corn starch has globular, polyhedral shapes with approximate diameters of 5–25 μm and in Figure 1 (c, d, e), no apparent deficiency or hint of surface damage after debranching and recrystallization. The TEM images in (Figure 1f, g, h) showed the well dispersed of StNPs with slight aggregation and diameter around 25-50 nm less than obtained from waxy maize (50–100 nm width and 80–120 nm length). StNPs were obtained following enzymolysis of native starch following recrystallization of linear glucans (DP about 12–60). The recrystallization of StNPs was done by combining linear glucans into double helices and forming

clusters with hydrogen bond, then rearranging the clusters into StNPs. Double helices were probably aggregated to nanoscale starch particles (25–50 nm, diameter) within 8 h of the recrystallization period after 8 h of debranching. Freeze drying has significantly influenced the production of dried starch nanoparticles. Particle size of more than 100 was due to aggregation of some particles [4].

3.1.2. StNPs Particles size.

The size distribution of StNPs was also measured using DLS. From Figure 2, the size ranged from 50 to 250 nm with about 100 nm as a mean size, which was larger than that measured by TEM. During DLS measurement, nanoparticles tend to agglomerate in aqueous state and give clustered particles size rather than individual particles. Unlike TEM, the findings of the DLS showed a broader nanoparticles size range; this method

cannot be used to differentiate between individual particles and agglomerates. The size of TEM was lower than that detected by DLS, and could be attributed to self-aggregation of nanoparticles [17].

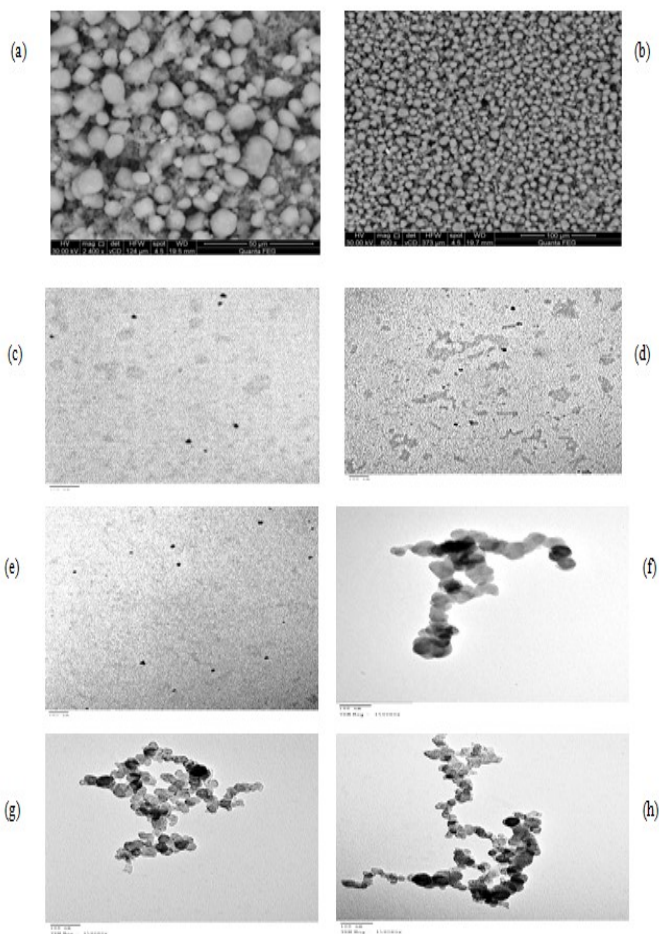


Figure 1. SEM images of native starch (a, b), of StNPs (c, d, e), and TEM images of StNPs (f, g, h).



Figure 2. Dynamic light scattering of: (a) StNPs, (b) after debranching and (c) recrystallization of short glucan units.

3.1.3. X-ray diffraction.

X-ray diffraction has been used to report the crystalline structure of starch nanoparticles and the effect of self-assembly technique on crystallinity. Native corn starch granules had a typical crystalline arrangement of type A, showing peaks of diffraction around 15.8, 16.9, 18.1, and 23.5 (2 hrs.) as in Figure 3, following previous findings [18]. There were no changes in the X-ray of StNPs sample as compared with native starch displayed a typical A-type crystalline structure with main diffraction peaks at $2\theta = 15.4, 17.1$ and 22.5 that may be due to the amylose content in corn starch 20-30% [1]. StNPs from native waxy maize with amylose content 1-5 % gives different results according to the temperature of recrystallization [4].

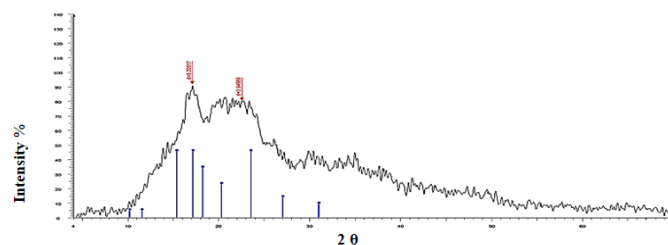


Figure 3. XRD of StNPs.

3.1.4. FT-IR spectra.

Native corn starch, StNPs, chitosan and chitosan-StNPs spectra are obtained in Figure 4. As appeared in Figure 4, broad bands from 3100 to 3700 cm^{-1} were attributed to the complex vibrational stretches associated with inter- and intra-molecular hydroxyl groups. For C – H stretches associated with ring methane hydrogen atoms, the bands 2925 and 2926 cm^{-1} were characteristic. The weak band of 2077 cm^{-1} was triggered by C-H and C-C vibration. The peak height at 1640 cm^{-1} was reduced and the width of the peak was boarded due to tightly-bound water. The bands from 1300 to 900 cm^{-1} resulted from C–O and C–C vibrational modes causing difficulty to assign individual bands. For native starch, three characteristic peaks of C–O bond stretching appeared between 933 and 1156 cm^{-1} . The skeletal mode vibrations of the 4-glycoside link (C – O – C) at a distance of 940 cm^{-1} are referred. The others at $1081, 1020,$ and 1156 cm^{-1} were characteristic for the C–O stretch anhydro glucose ring. In StNPs, the 1156 cm^{-1} and 1081 and 1067 cm^{-1} bands moved to a lower frequency and the 1020 cm^{-1} shifted to a higher frequency indicating that the molecular chains had chemical interactions. In hydrogen bonding of starch chains and being stronger than in native starch molecules, the peaks at $1156, 1081$ and 1020 cm^{-1} were 1150 and 1078 . The average was 1015 cm^{-1} . Such modifications revealed that pullulanase had deposited the native starch, which could increase the number of linear glucans [4]. For StNPs, chitosan and chitosan/StNPs, the FTIR spectra showed a broad band between 3600 cm^{-1} and 3100 cm^{-1} that ascribed to hydroxyl group (O-H) stretching vibrations in chitosan and starch backbone. In chitosan, the observed bands at 1650 cm^{-1} and 1570 cm^{-1} are attributed to carbonyl group (C=O) stretching and N-H bending of amide I groups. The bands at 1410 cm^{-1} and 1385 cm^{-1} are ascribed to methyl group (CH_3) symmetrical deformation mode. The broad band at 1150 cm^{-1} is attributed to the C-O stretching vibrations of chitosan. A new band was observed at 1644 cm^{-1} and belonging to the interaction between StNPs and chitosan during the drying process. Also, the bands at 1109 cm^{-1} and 1026 cm^{-1} were depicting C-O stretching and C-O-C bending in the network structure [14].

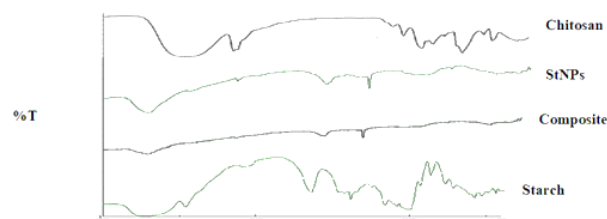


Figure 4. Starch, StNPs, composite and chitosan.

Investigation of an adsorbent based on novel starch/chitosan nanocomposite in extraction of indigo carmine dye from aqueous solutions

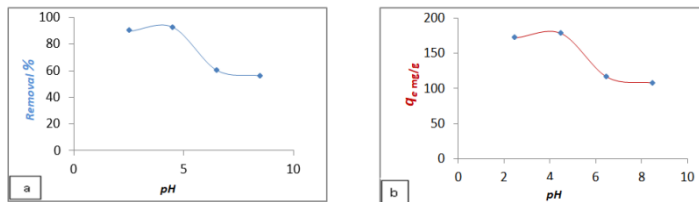


Figure 5 (a,b). Effect of pH on IC adsorption capacity and removal.

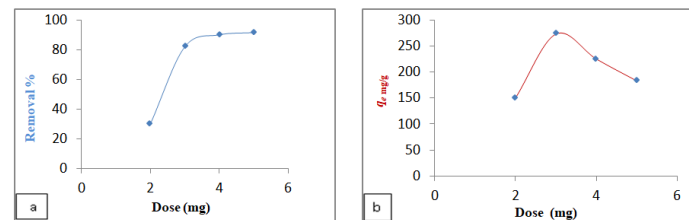


Figure 6 (a,b). Effect of adsorbent dose on IC adsorption capacity and removal.

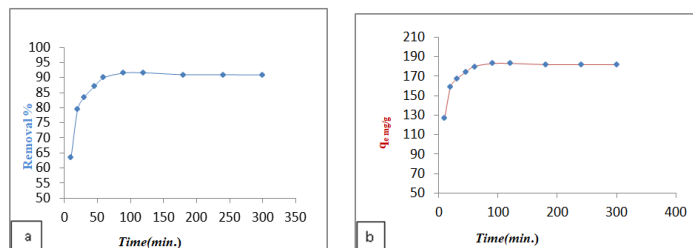


Figure 7 (a, b). Effect of contact time on IC adsorption capacity and removal.

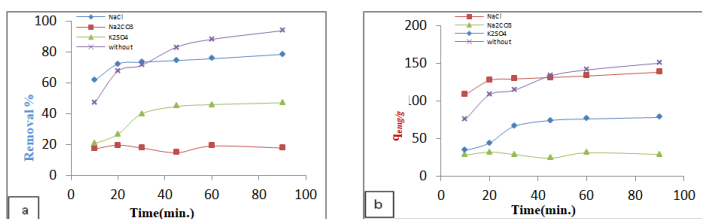


Figure 8 (a,b). Effect of inorganic salt on IC adsorption capacity and removal.

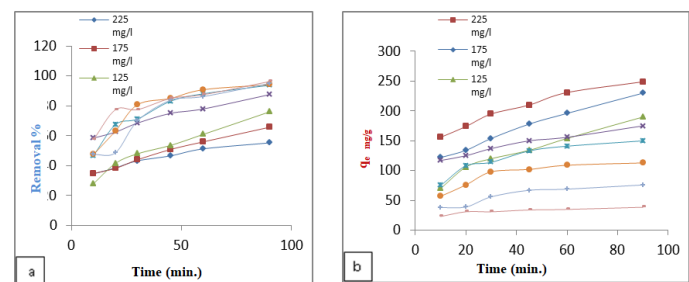


Figure 9 (a, b). Effect of initial concentration on IC adsorption capacity and removal.

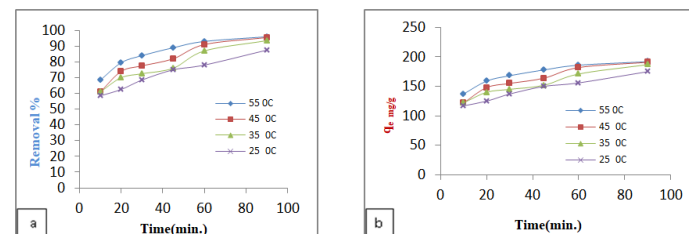


Figure 10 (a, b). Effect of temperature on IC adsorption capacity and removal.

3.2. Adsorption examination.

The adsorption of indigo carmine IC dye onto chitosan-StNPs composite involves ionic interaction between anionic sulfonyl (SO_3^-) groups of dissolved dye and the protonated amino (NH_3^+) groups of chitosan enhanced by hydrophobic/hydrophilic interaction of alkyl groups. For successful adsorption, dissociation

of dye molecules and activation of chitosan-StNPs composite functional groups is important for the electrostatic attraction between the existing species as illustrated in reaction I and II.

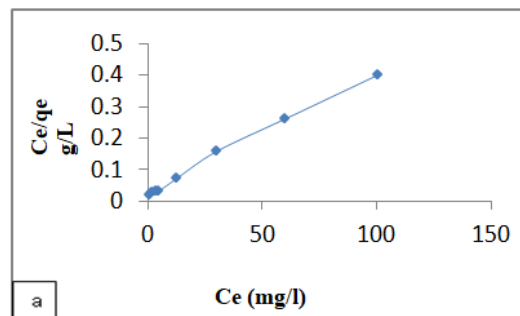


Figure 11a. Langmuir isotherm.

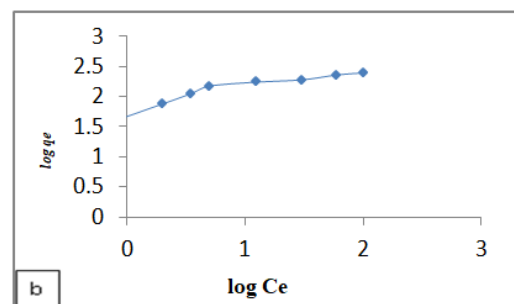


Figure 11b. Freundlich isotherm.

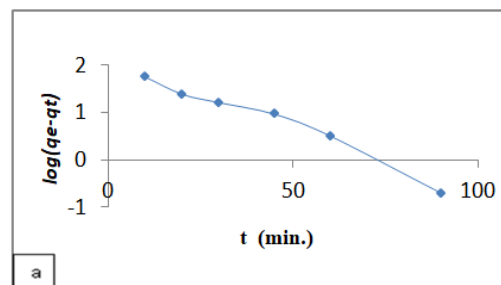


Figure 12a. pseudo first order.

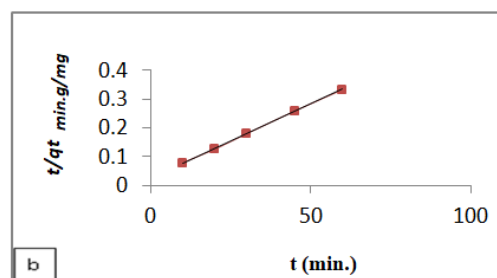


Figure 12b. Pseudo second order.

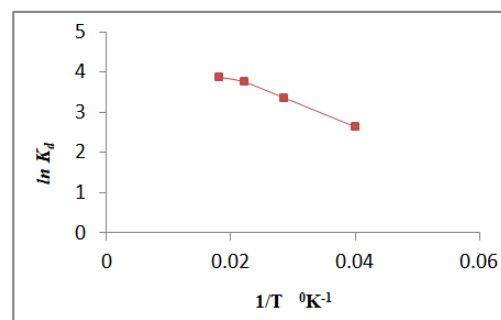
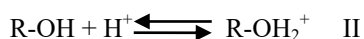
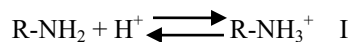


Figure 13. Vant Hoff $\ln K_d$ & $1/T$.

Reaction III indicates a dissociation of the coloring organisms into the water solution creating a sulfonyl group with anionic load. The adsorption process occurred due to electrostatic

interaction between the activated species of chitosan-StNPs composite and IC dye via the counter ions reaction represented in reaction IV [13].



Scheme 1. The binding of IC dye molecules onto surface.

3.2.1. Effect of pH.

The functional groups of existing species were highly affected by the pH value of IC dye solution. The amine groups have been protonated in the acidic medium and by counter ion reactions; negative IC dye ions were adsorbed by ion attraction as shown in Scheme 1 [13]. Figure 5 (a,b) demonstrated a healthy dye sorption at a different initial pH range from 2.5 to 8.5 for 100 mg / L, 50 mg / L and 25o C for 90 min. The dosage adsorbed was adsorbed. It was indicated at pH 4.8with maximum removal percentage of 92.7 % because of the protonated amino (NH³⁺) groups are raising the binding of the dye molecules. The dye percent of removal goes down from 92.7 % to 56.25 % as pH increased from 2.5 to 8.5. This decrease was because the number of protonated amino groups in the chitosan-StNP surface were decreased slowly and electrostatic contact between chitosan-StNPs and dye molecules was decreased [19-21].

3.2.2. Effect of adsorbent dose

The uptake of IC dye at constant initial dye concentration of 100 mg/L, pH 4.8 and temperature of 25 °C for 90 min. was estimated at a different composite dose (20-50mg) Figure 6 a. The uptake capacity of IC dye increased from 150 mg/g to 273.3 mg/g. This increase was due to an increase in adsorption sites as Ch-StNPs composite dose increased. Also, Figure 6 b, percentage removal of dye increased as adsorbent dose increased from 30 % to 91.5% with increasing adsorbent dose from 20 mg to m50g [22].

3.2.3. Effect of contact time.

The adsorption cycle was adsorbed at a steady dosage of 50 mg/L, pH 4.8 and 100 mg/L at a concentration of 25 °C. As shown in Figure 7 (a, b), as the touch period decreases, adsorption grows to 90 minutes. In the first 30 minutes, the first adsorption became quicker, then gradually to stabilize [13, 23].

3.2.4. Effect of presence of inorganic salts.

Evaluating the effect of inorganic salt was important factor as it is usually used for improvement dyeing process, study the effect of some salts on adsorption of dye onto Ch-StNPs composite adsorbate was carried out at constant initial dye concentration of 100 mg/L and temperature of 25 °C for 90 min. using 0.1 M NaCl, Na₂CO₃ and K₂SO₄ as shown in Figure 8 (a, b). CO₃²⁻ ions have higher inhibition effect on the adsorption of IC dye onto composite while SO₄²⁻ ions have middle effect and the lower effect on adsorption Cl⁻ ions. This effect may be attributed to the competitive of ions present on the dye and salts on adsorbate sites [24, 25].

3.2.5. Effect of initial dye concentration.

The high initial coloring concentration provided an important driving force to counteract mass transfer strengths of

colour, between the aqueous and solid phases, thus increasing sorption. The increase in initial color concentration creates more stress between color and adsorbents, thereby increasing the sorting process. The effect of the initial sorption dye was investigated at a constant solution pH 4.8 from 20 to 225 mg/L, while adsorbed doses 50 mg/L was investigated at 25 °C at different times before equilibrium. The findings are shown in Figure 9, a percentage of IC color removal decreased with increased initial coloration concentration, as predicted. Removal decreased from 96, 25 to 55,3% with the original concentration of 20 mg / L raised to 225 mg / L. Sorption efficiency was improved on the other side as the concentration of IC dye was due to the increased number of dye molecules as shown in Figure 9b. The results show that the initial concentration of IC coloration that decreases at higher levels was strongly adsorption dependent [26, 27].

3.2.6. Effect of temperature.

The adsorption capacity was examined at various temperatures (25, 35, 45, 55 °C) at constant pH 4.8, adsorbed dose 50 mg/L, initial dye concentration of 100 mg/L for 90 min.. Obtained results proved that removal of IC dye was increased with increasing temperature as represented in Figure 10 (a, b). The rise in sorption was attributed comparatively to the high number of active composite sites created with higher temperatures and decreased motion in film of the coloring molars as the temperature rose. This confirmed the connection between IC coloration molecules and a structure at higher temperatures [28].

3.3. Adsorption isotherm.

Adsorption device enhancements using isothermic models are powerful tools. The most famous models for this function are Langmuir and Freundlich. The isothermal Langmuir means that adsorbent has a homogeneous surface with a fixed equal sites adsorbing fixed number of adsorbate molecules. The isotherm of Freundlich defines the adsorption rule of the amorphous surface and provides the future formation of various monolayers. The different isotherms are explained by equations (3) and (4).

$$C_e/q_e = 1/bq_m + q_e/q_m \quad (3)$$

$$\log q_e = \log k_f + 1/n \log C_e \quad (4)$$

where q_e is the IC adsorption capacity (mg/g) at equilibrium and q_m is the monolayer adsorption capacity per unit mass of adsorbent (mg/g) and C_e is the IC concentration at equilibrium (mg/L). Vector b is the Langmuir constant (L / mg), k_F is the Freundlich constant (L / g), and the 1/n (dimensional-free) vector represents the surface heterogeneity of adsorption. As seen in Figure 11 (a, b), the experimental findings were not only Freundlich Isotherms, but also Langmuir and all parameters were calculated as shown in Table 1. The correlation coefficient (R²) was slightly larger for the adsorbent assay than for Freundlich isotherm. The action of IC adsorption on specific Adsorbents was observed as well [9, 29-31]. The parameter b refers to the interaction intensity between the adsorbent and the adsorbate. From Langmuir isotherm, it is possible to expect if the adsorption of IC of the adsorbent was favorable or not. The separation factor (RL) can be calculated using the following equation (5):

$$RL = 1/ (1 + bC_0) \quad (5)$$

RL value reveals the type of the isotherm to be favorable (0 < RL < 1), unfavorable (RL > 1), linear (RL = 1) or irreversible (RL =

0). It was 0.03 for the Ch-StNPs composite. Thus, the IC adsorption on both adsorbent samples is favorable [9].

3.4. Adsorption kinetics.

Adsorption kinetics gives important information about the mechanism of adsorption and permits comparing with different adsorbents under special operational conditions for similar applications. To investigate the IC adsorption in the chitosan-StNPs composite, experimental data were treated by pseudo-first-order and pseudo-second-order models as mentioned in equations (6) and (7).

$$\text{Log}(q_e - q_t) = \text{Log} q_e - k_1 t / 2.303 \quad (6)$$

$$t/q_t = 1/k_2 q_e^2 + t/q_e \quad (7)$$

where q_e and q_t are the IC adsorption capacity (mg/g) in the composite sample at equilibrium at any time (t). K_1 is the constant rate of the pseudo-first order extracted from the linear log plot slope of $(q_e - q_t)$ versus t as shown in Figure 12 a. K_2 is the rate constant of the pseudo-second order detected by the intercept linear plot of t / q_t versus t (Figure 12 b). Table 2 includes all of these factors and the linear coefficient of correlation (R^2). The theoretical value of q_e was determined using the second-order pseudo-model and was similar to the experiments. The q_e values determined with the first-order pseudo-model are not consistent with the test data. For this second kinetic model, the values of the correlation coefficient (R^2), which are strongly proof of IC adsorption in adsorption samples, were compared to 0.99 and preceded by second-order pseudo-cinematics. This model

guarantees that the IC adsorption operation is driven by a mechanism of chemisorption arising from valence forces through electron sharing or association between adsorbent and adsorbent specimens [32, 33].

3.5. Thermodynamic studies.

The thermodynamic behavior of IC dye sorption onto composite was investigated by evaluation of free Gibbs energy (ΔG°), enthalpy (ΔH°) and entropy (ΔS°) of the sorption process using Eq. (8), (9) and (10):

$$K_d = C_e / q_e \quad (8)$$

$$\text{Ln} K_d = -\Delta G / RT = -\Delta H / RT + \Delta S / R \quad (9)$$

$$\Delta G = \Delta H - T \Delta S \quad (10)$$

where, K_d is the distribution constant, R (8.314 J/mol K) the universal gas constant, C_e (mg/L) is the equilibrium concentration of dye on adsorbent, q_e adsorption capacity at equilibrium and T (K) the temperature. ΔS° and ΔH° were deduced from the slope and intercepted Van't Hoff plot of $\text{Ln} K_d$ vs. $1/T$ (Figure 13). ΔG° has been determined and all thermodynamic data are listed in Table 3. The adverse values of ΔG° confirmed spontaneous dye sorption. The decrease in ΔG° values was a result of the system's spontaneity a rise in temperature. It was indicated an endothermic sorption process ($\Delta H^\circ = +ve$). The value of ΔS° demonstrated randomness at the solid-solute interface indicating an adequate affinity of IC dyes to chitosan-StNPs with some structural changes in the adsorbate and adsorbent binding [13, 32, 34-36].

Table 1. Langmuir and Freundlich Isotherm for IC adsorption onto Ch-StNPs composite.

Adsorbent	T °C	q_e (mg/g)	Langmuir Isotherm			Freundlich Isotherm			
			q_m (mg/g)	b (L/mg)	R^2	Kf (L/g)	n	1/n	R^2
Ch-StNPs	25	249	256.4	0.18	0.9956	61.47	2.915	0.343	0.8712

Table 2. pseudo first and second order parameters for IC adsorption onto Ch-StNPs composite.

IC adsorption on composite		pseudo first order			pseudo second order		
c_0 (mg/L)	$q_{e \text{ exp}}$ (mg/g)	k_1	$q_{e \text{ cal}}$ (mg/g)	R^2	k_2	$q_{e \text{ cal}}$ (mg/g)	R^2
100	182	0.067	123.6	0.9717	987.68	196	0.9997

Table 3. Thermodynamic parameters for IC adsorption onto Chitosan/StNPs composite.

T (K)	ΔG (kJ mol ⁻¹)	ΔS (J mol ⁻¹ K ⁻¹)	ΔH (kJ mol ⁻¹)
298	-8.22	+140	33.5
308	-9.62		
318	-11.02		
328	-12.42		

4. CONCLUSIONS

Synthesis of starch nano-particles through enzymolysis procedure is considered the best way as time, outlet and environment friendly. Both TEM&SEM images show round and polyhedral shape of native starch, StNPs and nano sized of prepared StNPs. A novel adsorbent is obtained from StNPs and chitosan and examined for removal of indigo carmine dye from aqueous solution. The adsorption results showed that the highest color removal is 4.8, and 323 K for 90 min. The isothermic

adsorption was best fitted with Langmuir, which suggests that an adsorbent monolayer is formed on the adsorbent surface. Moreover, the adsorption of IC coloring colouring was following the pseudo-second-order kinetics which confirmed that the process was adsorbed by chemisorption. Thermodynamic calculations have proven spontaneous, endothermic and random adsorption processes.

5. REFERENCES

- Ni, S.; Zhang, H.; Dai, H.; Xiao, H. Starch-based flexible coating for food packaging paper with exceptional hydrophobicity and antimicrobial activity. *Polymers* **2018**, *10*, 1260-1267, <https://dx.doi.org/10.3390/polym10111260>
- ALI, SF Abdellah. Mechanical and thermal properties of promising polymer composites for food packaging applications.

- In: IOP Conference Series: Materials Science and Engineering. *IOP Publishing*, **2016**, 137, 012035, [doi:10.1088/1757-899X/137/1/012035](https://doi.org/10.1088/1757-899X/137/1/012035)
- Wang, H.; Feng, T.; Zhuang, H.; Xu, Z.; Ye, R.; Sun, M. A review on patents of starch nanoparticles: Preparation, applications, and development. *Recent patents on food, nutrition*

- & agriculture **2018**, *9*, 23-30, <https://doi.org/10.2174/2212798410666180321101446>.
4. Tran, T.; Athanassiou, A.; Basit, A.; Bayer, I. Starch-based bio-elastomers functionalized with red beetroot natural antioxidant. *Food Chemistry* **2017**, *216*, 324-333, <http://dx.doi.org/10.1016/j.foodchem.2016.08.055>.
5. Salam, A.; Lucia, L.; Jameel, H. Synthesis, Characterization, and Evaluation of Chitosan-Complexed Starch Nanoparticles on the Physical Properties of Recycled Paper. *ACS. App. Mater. Inter.* **2013**, *5*, 11029-11037, <http://dx.doi.org/10.1021/am403261d>.
6. Chang, R.; Tian, Y.; Yu, Z.; Sun, C.; Jin, Z. Preparation and characterization of zwitterionic functionalized starch nanoparticles. *International Journal of Biological Macromolecules* **2020**, *142*, 395-403, <https://doi.org/10.1016/j.ijbiomac.2019.09.110>.
7. El-Feky, G.; El-Rafie, M.; El-Sheikh, MA.; E El-Naggar, M.; Hebeish, A. Utilization of Crosslinked Starch Nanoparticles as a Carrier for Indomethacin and Acyclovir Drugs. *J. Nanomed. Nanotechnol.* **2015**, *6*, 1, <http://dx.doi.org/10.4172/2157-7439.1000254>.
8. Gomes, R.; Azevedo, N.; Pereira, A.; Muniz, E. Fast dye removal from water by starch-based composites. *J. Coll. and Interface Sci.* **2015**, *454*, 200-209, <http://dx.doi.org/10.1016/j.jcis.2015.05.026>.
9. Gad, E.S.; Owda, M.; Abdelhai, F. A Novel Starch Nanoparticle Citrate based Adsorbent for removing of Crystal Violet dye from aqueous solution. *Egyptian Journal of Chemistry* **2019**, <https://doi.org/10.21608/EJCHEM.2019.16593.2013>.
10. Qiao, D.; Liu, H.; Yu, L.; Bao, X.; Simon, G., Petinakis, E.; Chen, L. Preparation and characterization of slow-release fertilizer encapsulated by starch-based superabsorbent polymer. *carbohydr. Polymer* **2016**, *147*, 146-154, <http://dx.doi.org/10.1016/j.carbpol.2016.04.010>.
11. Islam, S.; Bhuiyan, M.; Islam, M.; Chitin and Chitosan: Structure, Properties and Applications in Biomedical Engineering. *J Polym Environ.* **2017**, *25*, 854-866, <http://dx.doi.org/10.1007/s10924-016-0865-5>.
12. Ngwabebhoh, F.; Gazi, M.; Oladipo, A. Adsorptive removal of multi-azo dye from aqueous phase using a semi-IPN superabsorbent chitosan-starch hydrogel. *Chem. Eng. Research and Design* **2016**, *112*, 274-288, <https://doi.org/10.1016/j.cherd.2016.06.023>.
13. Tanhaei, B.; Ayati, A.; Sillanpää, M. Magnetic xanthate modified chitosan as an emerging adsorbent for cationic azo dyes removal: Kinetic, thermodynamic and isothermal studies. *International journal of biological macromolecules* **2019**, *121*, 1126-1134, <https://doi.org/10.1016/j.ijbiomac.2018.10.137>.
14. Sun, Q.; Li, Y.; Li, Y.; Li, F.; Zhang, W.; Chen, S.; Cui, F. Optimisation of compatibility for improving elongation at break of chitosan/starch films. *RSC advances* **2019**, *9*, 24451-24459, <https://doi.org/10.1039/C9RA04053F>.
15. Navarro, M.; Soukup, K.; Jandová, V.; Gómez, M.; Solis, L.; Cruz, F.; Cruz, F. Starch/chitosan/glycerol films produced from low-value biomass: effect of starch source and weight ratio on film properties. *Journal of Physics: Conference Series, IOP Publishing* **2019**, *1173*, [doi:10.1088/1742-6596/1173/1/012008](https://doi.org/10.1088/1742-6596/1173/1/012008).
16. Liu, C.; Qin, Y.; Li, X.; Sun, Q.; Xiong, L.; Liu, Z. Preparation and characterization of starch nanoparticles via self-assembly at moderate temperature. *Inter. J. Biologica. Macromolec.* **2016**, *84*, 354-360, <http://dx.doi.org/10.1016/j.ijbiomac.2015.12.040>.
17. Alila, S.; Aloulou, F.; Thielemans, W.; Boufi, S. Sorption potential of modified nanocrystals for the removal of aromatic organic pollutant from aqueous solution. *Industrial Crops and Products* **2011**, *33*, 350-357, <http://dx.doi.org/10.1016/j.indcrop.2010.11.010>.
18. Kyzas, G.; Bikiaris, D. Recent Modifications of Chitosan for Adsorption Applications: A Critical and Systematic Review. *Mar. drugs* **2015**, *13*, 312-337, <https://doi.org/10.3390/md13010312>.
19. Wang, Z.; Xiang, B.; Cheng, R.; Li, Y. Behaviors and mechanism of acid dyes sorption onto diethylenetriamine-modified native and enzymatic hydrolysis starch. *J. Hazard. Mater.* **2010**, *183*, 224-232, <http://dx.doi.org/10.1016/j.jhazmat.2010.07.015>.
20. Iqbal, J.; Wattoo, F.; Wattoo, M.; Malik, R.; Tirmizi, S.; Imran, M. Adsorption of acid yellow dye on flakes of chitosan prepared from fishery wastes. *Arab. J Chem.* **2011**, *4*, 389-395, <http://dx.doi.org/10.1016/j.arabjc.2010.07.007>.
21. Haldorai, Y.; Shim, J. An efficient removal of methyl orange dye from aqueous solution by adsorption onto chitosan / MgO composite: A novel reusable adsorbent. *Appl. Surface Sci.* **2014**, *292*, 447-453, <http://dx.doi.org/10.1016/j.apsusc.2013.11.158>.
22. Zhao, P.; Zhang, R.; Wang, J. Adsorption of methyl orange from aqueous solution using chitosan/diatomite composite. *Water Sci. Technol.* **2017**, *75*, 1633-1642, <http://dx.doi.org/10.2166/wst.2017.034>.
23. Yuksel, A. Hydrothermal Degradation of Congo red in Hot Compressed Water and its Kinetics. *J Chem. Eng. Process Technol.* **2013**, *4*, 179, <http://doi.org/10.4172/2157-7048.1000179>.
24. Zhu, Z.; Zhang, M.; Liu, F.; Shuang, C.; Zhu, C.; Zhang, Y.; Li, A. Effect of polymeric matrix on the adsorption of reactive dye by anion-exchange resins. *J. of the Taiwan Institute of Chem. Eng.* **2016**, *21*, 50, <http://dx.doi.org/10.1016/j.jtice.2016.01.017>.
25. Jabbar, A.; Hadi, A.; Sami, F. Removal of Azo Dye from Aqueous Solutions using Chitosan. *Oriental J. Chem.* **2014**, *30*, 571-575, <http://dx.doi.org/10.13005/ojc/300222>.
26. Saha, T.; Bhoumik, N.; Karmake, S.; Ahmed, M.; Ichikawa, H.; Fukumori, Y. Adsorption Characteristics of Reactive Black 5 from Aqueous Solution onto Chitosan. *Clean – Soil, Air, Water* **2011**, *39*, 984-993, <http://dx.doi.org/10.1002/clen.201000315>.
27. Sarkar, K.; Banerjee, S.; Kundu, P. Removal of Anionic Dye in Acid Solution by Self Crosslinked Insoluble Dendronized Chitosan. *Hydrol Current Res* **2012**, *3*, 3, <http://dx.doi.org/10.4172/2157-7587.1000133>.
28. Simanaviciute, D.; Liudvinaviciute, D.; Klimaviciute, R.; Rutkaite, R. Cross-linked cationic starch derivatives for immobilization of chlorogenic acid. *Euro. Polymer J.* **2017**, *93*, 833-842, <https://doi.org/10.1016/j.eurpolymj.2017.02.022>.
29. Islam, T.; Peng, C. Synthesis of carbon embedded silica and zeolite from rice husk to remove trace element from aqueous solutions: characterization, optimization and equilibrium studies. *Separation Science and Technology* **2019**, 1-14, <https://doi.org/10.1080/01496395.2019.1658781>.
30. Kumari, S; Yadav, S.; Yadav, B. Synthesis and modification approaches for starch nanoparticles for their emerging food industrial applications: A review. *Food Research International* **2019**, <https://doi.org/10.1016/j.foodres.2019.108765>.
31. Jain, A.; Khar, R.; Ahmed, F.; Diwan, P. Effective insulin delivery using starch nanoparticles as a potential trans-nasal muco adhesive carrier. *Euro. J. Pharm. and Biopharm* **2008**, *69*, 26-435, <http://dx.doi.org/10.1016/j.ejpb.2007.12.001>.
32. Xu, Y.; Yan, X. Adsorption of Cr (VI) onto the Cross-linked Cationic Starch and the Establishment of the Adsorption Isotherm and Kinetic Equation. *Advanced Materials Research* **2012**, *518-523*, 285-288, <http://dx.doi.org/10.4028/www.scientific.net/AMR.518-523.285>

Investigation of an adsorbent based on novel starch/chitosan nanocomposite in extraction of indigo carmine dye from aqueous solutions

33. Jiang, S.; Yu, Z.; Hu, H.; Lv, J.; Wang, H.; Jiang, S. Adsorption of procyanidins onto chitosan-modified porous rice starch. *LWT-Food Sci. and Tech.* **2017**, *84*, 10-17, <https://doi.org/10.1016/j.lwt.2017.05.047>
34. Alamo, N.; Espinosa, R.; Ríos, M.; Rivas, J.; Arce, R.; Gaitán, B. Adsorption behavior of copper onto a novel modified chitosan material: thermodynamic study. *Desalin. and water Treat.* **2016**, *57*, 1-9, <http://dx.doi.org/10.1080/19443994.2016.1143881>.
35. Chen, Y.; Liu, S.; Wang, G. A kinetic investigation of cationic starch adsorption and flocculation in kaolin suspension, *Chem. Eng. J.* **2007**, *133*, 325-333, <http://dx.doi.org/10.1016/j.cej.2007.02.019>.
36. Phanthuwongpakdee, J.; Babel, S.; Kaneko, T. Natural Adsorbents for Removal of Different Iodine Species from Aqueous Environment: A Review. In: *Recent Trends in Waste Water Treatment and Water Resource Management*. Springer, Singapore 2020; pp. 171-198, https://doi.org/10.1007/978-981-15-0706-9_17.



© 2020 by the authors. This article is an open access article distributed under the terms and conditions of the Creative Commons Attribution (CC BY) license (<http://creativecommons.org/licenses/by/4.0/>).